Journal of Thermal Analysis and Calorimetry, Vol. 86 (2006) 2, 351–357

SYNTHESIS, CHARACTERIZATION, SPECTROSCOPY AND THERMAL ANALYSIS OF RARE EARTH PICRATE COMPLEXES WITH *L*-LEUCINE

*T. S. Martins, J. R. Matos, G. Vicentini and P. C. Isolani**

Instituto de Química, Universidade de São Paulo, CP 26077, 05513-970 São Paulo, Brazil

Rare earth picrate complexes with *L*-leucine (Leu) were synthesized and characterized. Elemental analysis (CHN), EDTA titrations and thermogravimetric data suggest a general formula $RE(pic)_3 2Leu \cdot 5H_2O$ (*RE*=La–Lu, Y and *pic*=picrate). IR spectra indicate the presence of water and suggest that *L*-leucine is coordinated to the central ion through the nitrogen of the aminogroup. The absorption spectrum of the solid Nd compound indicates that the metal-ligand bonds show a weak covalent character. Emission spectra and biexponential behavior of the luminescence decay of the Eu compound suggest the existence of polymeric species. Thermal analysis results indicate that all the compounds present a similar behavior, with five major thermal decomposition steps. The final products are rare earth oxides. A slow heating rate is necessary to observe all decomposition steps.

Keywords: *complexes, L-leucine, luminescence, rare earth picrates, thermal analysis*

Introduction

Rare earths are very suitable for a variety of industrial and biological applications, due mainly to their spectroscopic and magnetic properties. In industry, the applications of rare earths are many, such as in catalysis, phosphors, magnetic materials, glasses and lasers [1–14]. In biological systems, the use of trivalente rare earth ions has attracted a great deal of interest. In these systems, they usually are used as luminescent probes in the investigations of binding sites in proteins and other biomolecules, labels in immunoassays and in non-invasive tests [15–19].

Studies of the coordination chemistry of rare earth ions with amino acids have been of great importance on biological systems. Amino acids are important compounds and they participate in many biochemical processes essential to living systems; furthermore, some rare earth ions have excellent luminescence properties. For these reasons the interaction lanthanide-amino acids has been in the center of attention of many investigations [20–25]. However, in the literature, no complexes of *L*-leucine with rare earth picrates have been reported to date.

Complexes containing picrates as counter ions have been investigated systematically in our laboratories. Rare earth picrate complexes with several organic neutral ligands (including the amino acids glycine, lysine and arginine), involving synthesis, characterization, studies of properties and structures have been reported [20, 21, 26–33]. The presence of the picrate anion (2,4,6-trinitrophenolate) in these coordination compounds is expected to enhance the luminescence properties of these materials, because this anion acts as a luminescence antenna, absorbing and transferring energy efficiently to the rare earth ions and consequently increasing their luminescence [8, 15, 20, 21, 26–32].

Leucine (2-amino-4-methyl pentanoic acid) is an aliphatic monoamino monocarboxylic acid and exists predominantly as zwitterion. This amino acid is a branched chain essential amino acid that has important roles in protein and glucose metabolism, neurotransmitter synthesis and lymphoid tisssue metabolism. Leucine has an isoelectric point (pI) of ~5.98 and its pK_a values are 2.36 to COOH (pK_1) and 9.60 to NH_3^+ (pK_2) [34, 35].

In this paper, we describe the synthesis, characterization, spectroscopy and thermal analysis of rare earth picrate complexes with *L*-leucine.

Experimental

The complexes of rare earth picrates, $RE(pic)_3 \cdot xH_2O$, with *L*-leucine were prepared after extensive preliminary tests to which it was developed a preparation route to the new complexes; this route is according to the following: *L*-leucine (Sigma, purity above 98%, used without purification) in a molar ratio 1:2 (salt:ligand) was dissolved in ethanolic solution (50%) heated at 333 K and to this solution the rare earth picrate (solid) were added; this mixture was stirred at room temperature (298 K) for several days and only af-

* Author for correspondence: pcisolan@iq.usp.br

1388–6150/$20.00

Akadémiai Kiadó, Budapest, Hungary
Springer, Dordrecht, The Netherlands

ter about a week it was observed the formation of the initial precipitates. Total precipitation was observed after about two weeks. The precipitates (new compounds) were filtered and dried in a vacuum desiccator over anhydrous calcium chloride at room temperature.

The compounds were characterized by complexometric titration of the rare earth ions with standardized EDTA solutions using xylenol orange as indicator [36] and CHN microanalytical procedures using a PerkinElmer analyzer (model 240). Infrared absorption spectra were recorded in the range 4000–400 cm^{-1} in KBr pellets, using a Bomem MB-100 FT spectrometer. Conductance measurements in acetone and nitromethane were carried out at 298.00±0.02 K, using an apparatus composed of a resistance box, a pointer galvanometer and a cell (K_{cell}=0.1223 cm^{-1}), from Leeds and Northrup. Absorption spectra of the neodymium compound were obtained in a Zeiss DMR-10 spectrophotometer in the solid state at room temperature using a silicone mull in a 0.5 mm cell. Excitation and luminescence spectra of the gadolinium, terbium and europium compounds were recorded with a SPEX-Fluorolog-1681 spectrofluorimeter; luminescence decay profiles were measured with an SPEX 1934D phosphorimeter accessory coupled to a SPEX-Fluorolog FL 212 spectrofluorimeter at room temperature and 77 K. X-ray diffraction powder patterns were obtained on a Miniflex Rigaku diffractometer, with CuK_α (λ=1.5418 Å) radiation, in the range 5 to 60° (2θ).

TG/DTG curves were obtained on a Shimadzu TGA-50 thermobalance in the temperature range 298 to 1173 K with heating rates of 2 and 10 K min^{-1}, under dynamic air and nitrogen atmospheres (50 mL min^{-1}), using platinum crucibles with ca. 1.5 mg (10 K min^{-1}) and ca. 2 mg (2 K min^{-1}) samples. DSC curves were obtained on a Shimadzu DSC-50 cell using partially closed aluminum crucibles with ca. 1.5 mg of samples, under dynamic nitrogen atmosphere (100 mL min^{-1}) in the temperature range 298 to 673 K and with the same heating rates used for TG. The DSC cell was calibrated with indium (*m.p*. 429.6 K and ΔH_{fusion}=28.54 J g^{-1}) and zinc (*m.p*. 692.6 K).

Results and discussion

According to CHN analyses, EDTA titrations (%RE^{3+}) and thermogravimetry (Table 1) a general composition $RE(pic)_3 2Leu \cdot 5H_2O$ [*RE*=La–Lu (except Pm), Y; *pic*=picrate and *Leu*=*L*-leucine] was evidenced. The yellow compounds (due to the picrate anion) display also the superimposed characteristic hues of the respective RE^{3+} ions. They are crystalline powders, odorless, slightly hygroscopic, soluble in water, acetone, ethanol, methanol, nitromethane and slightly soluble in acetonitrile. Conductance measurements in acetone solution (10^{-3} mol L^{-1}) at 298.00±0.02 K (Table 1), presented values between 49 and 89 S cm^{-1} mol^{-1}, showing that all complexes behave as non-electrolytes [37].

According to X-ray patterns the compounds may be grouped into three isomorphous series, the first corresponding to La–Nd (strongest reflections at 2θ=15.4, 23.1, 28.6 and 41.7°), the second to Gd and Tb (6.3, 17.1, 25.1 and 42.4°) and the third to Ho-Lu and Y complexes (6.6, 10.9, 17.0, 20.5 and 29.3°). Sm, Eu and Dy complexes are not isomorphous and they do not belong to these series. Several attempts to obtain single crystals were unsuccessful.

All infrared spectra are similar and present as a general characteristic a shift of the ν_{NH} band of *L*-leucine to lower frequencies (3190 and 3035 cm^{-1}) with relation to the free ligand (3382 and 3061 cm^{-1}). This band shift to lower frequencies and the disappearance of the bands associated with the zwitterion structure (combination bands at 2127 cm^{-1}, characteristic of NH_3^+ groups of the amino group of free *L*-leucine) in the complexes, suggest that *L*-leucine is coordinated to the central ion through the nitrogen of the amine group. The infrared absorption spectrum of free *L*-leucine shows the asymmetric ($\nu_{as(COOH)}$) and symmetric stretching ($\nu_{s(COOH)}$) bands, located at 1582 and 1409 cm^{-1}, respectively. These vibrations in the complexes ($\nu_{as(COOH)}$~1571 cm^{-1} and $\nu_{s(COOH)}$~1430 cm^{-1}) do not present significant changes with relation to the free ligand, suggesting that the oxygen atom of the carboxylic group is not used in the ligand-metal ion bonding and that it is possibly bonded to water molecules through hydrogen bonds [20, 21, 38–43]. Bands due to the picrate ion at ~1273 cm^{-1} (ν_{CO}), ~1625, 1552 and 1500 cm^{-1} ($\nu_{as(NO_2)}$), ~1366 and 1335 cm^{-1} ($\nu_{s(NO_2)}$) were observed in the IR spectra. The bands attributed to NO_2 stretching are indicative of the existence of different types of nitro-groups and that at least in part the picrate anions are coordinated as bidentate ligands through the phenoxo group and one oxygen of an *ortho*-nitro group [20, 21, 27–30]. Broad bands around 3400 cm^{-1} are attributed to H_2O (ν_1 and ν_3), indicating the presence of water molecules in these complexes.

The visible absorption spectrum of the neodymium complex was recorded in the 560–610 nm region corresponding to the hypersensitive $^2G_{7/2}$, $^4G_{5/2} \leftarrow {}^4I_{9/2}$ transition. From Simpson's rule [44] it was possible to obtain the baricenter of this transition (17176 cm^{-1}), which allowed the calculation of the following parameters by comparison with data of standard Nd^{3+}:LaF_3 (17.329 cm^{-1}): nephelauxetic parameter (β=0.991), covalent factor ($b^{1/2}$=0.067) and Sinha's parameter (δ=0.908). These values suggest the presence of a small covalent character for the metal-ligand bonds.

Table 1 Analytical data for $RE(pic)_3 2Leu \cdot 5H_2O$ compounds and conductance measurements in acetone solution (10^{-3} mol L^{-1})

RE	*RE*/%		C/%		H/%		N/%		H_2O/%		RE_2O_3[c]/%		Λ_M/S cm^2 mol^{-1}
	calc.	exp.[a]	calc.	exp.	calc.	exp.	calc.	exp.	calc.	exp.[b]	calc.	exp.[c]	
La	11.8	11.3	30.6	30.0	3.6	3.5	13.1	13.0	7.7	7.7	13.9	12.4	62.9
Ce	11.9	11.9	30.6	30.5	3.6	3.6	13.1	13.9	7.7	7.7	14.6	14.3	48.7
Pr	12.0	12.3	30.6	30.5	3.5	3.9	13.1	13.2	7.6	7.6	13.3	13.7	53.3
Nd	12.2	12.3	30.5	30.0	3.6	3.5	13.0	13.0	7.6	7.7	14.2	14.0	49.7
Sm	12.7	12.7	30.3	29.0	3.5	3.1	13.0	13.3	7.6	7.6	14.7	18.4	33.8
Eu	12.8	12.3	30.3	30.4	3.6	3.8	13.0	12.9	7.6	7.7	14.8	18.3	62.3
Gd	13.2	13.2	30.2	31.0	3.6	3.8	12.9	12.4	7.5	7.6	15.2	15.5	66.4
Tb	13.3	13.6	30.5	30.0	3.5	3.4	12.9	12.3	7.5	8.0	15.6	15.0	67.4
Dy	13.5	13.9	30.0	30.6	3.6	3.6	12.8	12.8	7.5	7.6	15.6	15.4	74.0
Ho	13.7	13.5	30.0	29.4	3.5	3.5	12.8	12.0	7.5	7.8	15.7	16.0	77.8
Er	13.9	13.4	30.0	30.8	3.5	3.6	12.8	12.5	7.5	7.6	15.9	15.4	80.0
Tm	14.0	14.1	29.9	30.0	3.5	3.5	12.8	12.8	7.5	7.5	16.0	15.8	84.0
Yb	14.3	14.1	29.8	30.1	3.5	3.7	12.7	12.5	7.4	7.1	16.3	16.3	87.0
Lu	14.4	14.6	29.7	30.0	3.5	3.9	12.7	12.3	7.4	7.7	16.4	14.8	89.0
Y	7.9	7.7	32.0	32.9	3.8	4.1	13.7	13.3	8.0	8.2	10.0	10.7	68.0

[a]Complexometric titration with EDTA, [b]TG data analysis for dehydration and residues (2 K min^{-1}), [c]CeO_2, Pr_6O_{11} and Tb_4O_7

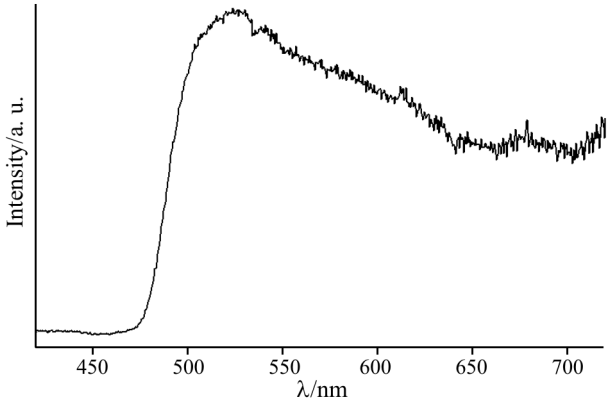

Fig. 1 Emission spectrum of the $Gd(pic)_3 2Leu \cdot 5H_2O$ complex at 77 K

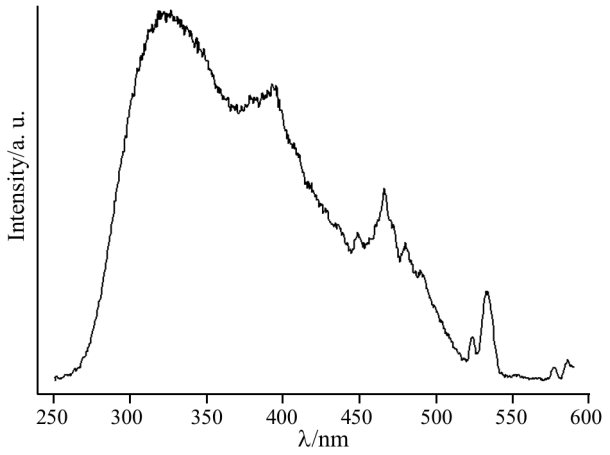

Fig. 2 Excitation spectrum of the $Eu(pic)_3 2Leu \cdot 5H_2O$ complex at room temperature

The luminescence spectrum of the $Gd(Pic)_3 2Leu \cdot 5H_2O$ complex (Fig. 1) at 77 K was recorded in the spectral range from 420 to 720 nm under excitation at 350 nm. This emission spectrum shows a wide phosphorescence emission band centered around 527 nm. This band is attributed to the picrate anion emission. Owing to the large energy gap (ca. 32000 cm^{-1}) between the $^8S_{7/2}$ ground state and first $^6P_{7/2}$ excited of the Gd^{3+} ion, this trivalent ion cannot accept any energy from the excited triplet estate of the organic ligand; for that reason, this spectrum was used to calculate the value of the lowest triplet state of the picrate ligand. The energy level of the triplet state of this ligand is around 18.975 cm^{-1}. For the terbium complex no luminescence is observed for Tb^{3+} ion at room temperature and 77 K; this can be due to the lowest excited energy levels of Tb^{3+} ion ($^5D_4$~20400 cm^{-1}) to be located above the excited triplet energy levels of the ligand. As a consequence, energy transfer from the ligands to trivalent terbium ion is not possible. In the spectral range 420 to 720 nm of this complex at room temperature like the gadolinium complex only a wide emission band attributed to picrate anion emission is observed.

The excitation spectrum for solid $Eu(pic)_3 2Leu \cdot 5H_2O$ complex (Fig. 2) was recorded in the spectral range from 250 to 590 nm at room temperature and with the emission monitored on the $^5D_0 \rightarrow {}^7F_2$ transition at 613 nm. As in other picrate complexes, this excitation spectrum presents a very broad band, evidencing the 'antenna effect' of the picrate ligands indicating that this anion is a good sensitizer for Eu^{3+} luminescence.

The emission spectra of the europium compound in the solid state at room temperature (298 K) and 77 K are similar, but at low temperature it is better resolved (Fig. 3). In the spectrum obtained at 77 K in the region of the $^5D_0 \rightarrow {}^7F_0$ transition one broad peak was observed at 577.5 nm; for $^5D_0 \rightarrow {}^7F_1$ three peaks were observed at 586.0, 591.2 and 593.3 nm; for $^5D_0 \rightarrow {}^7F_2$ two peaks (612.2 and 615.6 nm) and one shoulder (621.3 nm) were observed and for $^5D_0 \rightarrow {}^7F_4$ four peaks (687.9, 690.9, 693.0 and 695.7 nm) were observed too. The existence of a $^5D_0 \rightarrow {}^7F_0$ transition indicates that only C_{nv}, C_n and C_s symmetries are possible around the central Eu^{3+} ion [45]. As broad bands for $^5D_0 \rightarrow {}^7F_J$ (J=0, 1, 2 and 4) transitions were observed and the $^5D_0 \rightarrow {}^7F_0$ transition (at 77 K) has a 40 cm^{-1} half width, these results suggest the probable existence of polymeric species; that is in agreement with the biexponential decay of this luminescence [46]. The luminescence decay curve of the $^5D_0$ excited state of Eu^{3+} ion for solid $Eu(pic)_3 2Leu \cdot 5H_2O$ was obtained at 298 and 77 K. These curves fit very well to double-exponential curves with correlation coefficients of 0.9994–0.9996. Values of the lifetimes were calculated to be: τ_1=83.8 μs and τ_2=334.5 (298 K); τ_1=401.0 μs and τ_2=1284.8 μs (77 K).

Figure 4 shows TG/DTG and DSC curves of neat *L*-leucine. TG/DTG curves show only one step mass

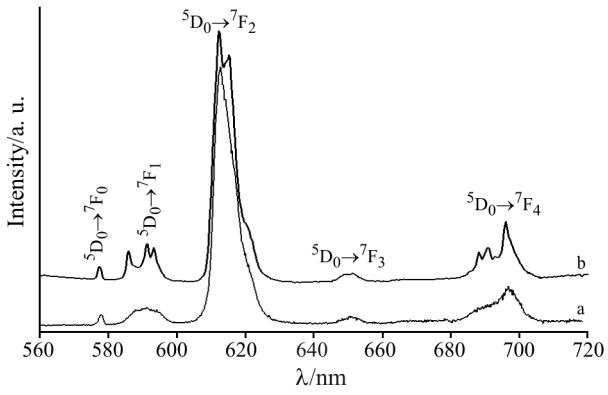

Fig. 3 Emission spectra of the $Eu(pic)_3 2Leu \cdot 2H_2O$ complex at a – 298 and b – 77 K

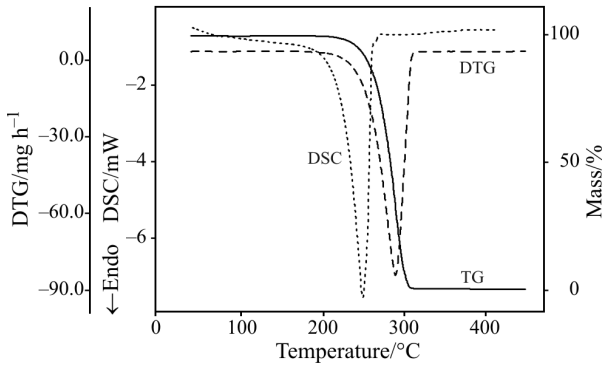

Fig. 4 TG/DTG and DSC curves of *L*-leucine obtained in dynamic nitrogen atmosphere (50 and 100 mL min^{-1}, respectively), heating rate 10 K min^{-1} and ca. 2.5 mg for both samples

loss (Δm=100%) between 485–588 K (T_{onset}=516 K and T_{peak}=563 K). Visual observation of the material under slow heating indicated that sublimation occurs. This event is characterized in DSC by an endothermic peak (T_{onset}=485 K, T_{peak}=524 K and $\Delta H_{sublimation}$= 148.1 kJ mol^{-1}). It was observed that the endothermic peak of *L*-leucine at 524 K disappears in the complexes RE(pic)$_3$2Leu·5H$_2$O indicating that they do not have free *L*-leucine. This modification in the DSC curve confirms that new compounds were formed; in other words, the prepared complexes are not a simple mixture of RE(pic)$_3$·*x*H$_2$O and *L*-leucine. Figure 5 shows TG/DTG and DSC curves of Er(pic)$_3$2Leu·2H$_2$O complex as a representative of the series.

All complexes exhibit a similar thermoanalytical profile. TG/DTG curves show one event of mass loss (7.6%) in the temperature range 298–403 K relative to elimination of five water molecules. Once dehydrated, the anhydrous compounds are stable up to 443 K and the thermal decomposition of these species

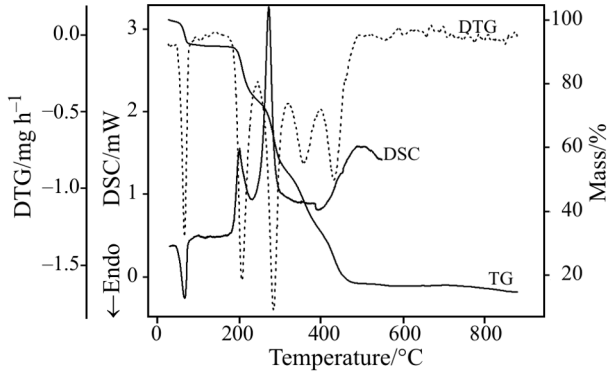

Fig. 5 TG/DTG and DSC curves of the Er(pic)$_3$2Leu·5H$_2$O complex obtained in dynamic air (50 mL min^{-1}) and nitrogen atmospheres (100 mL min^{-1}), respectively, heating rate 2 K min^{-1} and ca. 2 mg for both samples

in the temperature range 443 to 773 K occurs in four well-defined steps, reflecting in the DTG curves as can be seen in Fig. 5. The first mass loss after dehydration in the temperature range 443–513 K represents 17% of the total mass of the complexes. From stoichiometry calculations it can be attributed to the release of one picrate molecule. The second one (513–593 K) corresponds to 22.4%, attributed to the release of the leucine ligands. A step between 593 and 673 K (18.8%) can be attributed to the release of the second picrate molecule and the last one (673–1173 K) that represents 18.8% of the total mass of the adducts was attributed to the release of the third picrate molecule; however between 673 and 1173 K the loss mass is also due to elementary carbon elimination. This carbon is formed in the previous steps. These assumptions were corroborated by microanalytical procedures and IR spectroscopy.

For all compounds, the final thermal decomposition products were the respective oxides, RE_2O_3 (*RE*=La, Nd, Sm–Gd, Dy–Lu and Y), CeO_2, Pr_6O_{11} and Tb_4O_7, as evidenced by X-ray powder diffraction analyses of samples obtained by heating small quantities of the complexes at 1173 K in an oven. These X-ray patterns are identical to the ones of the respective oxides calcinated at 1173 K.

All thermal events observed in DSC curves in the temperature range 298 to 673 K (heating rate 10 K min^{-1}) are in accord with those observed in TG/DTG curves. The DSC curve for Er(pic)$_3$2Leu·5H$_2$O shows one endothermic event in the temperature range 298–393 K (ΔH=294.7 kJ mol^{-1}) corresponding to the release of water molecules. Besides, it also exhibits two exothermic peaks assigned to thermal decomposition of the complex. The first exothermic peak in the temperature range 443 to 506 K presents an enthalpy of –447.3 kJ mol^{-1} and the second one in the temperature range 506 to 673 K present an enthalpic value of –1141.1 kJ mol^{-1}. TG/DTG and DSC curves for all RE(pic)$_3$2Leu·5H$_2$O presented similar profiles. TG and DSC results for all complexes are summarized in Table 2.

It is important to mention that small amounts of material were used in all thermal analysis experiments due to the explosive properties of the picrates and, furthermore, the furnace atmosphere (N_2 and air) does not influence the decomposition processes of the compounds. However, for TG/DTG curves the heating rate (2 or 10 K min^{-1}) has an influence. TG/DTG curves obtained at heating rate of 10 K min^{-1} for all complexes show four steps of mass loss, whereas at heating rate of 2 K min^{-1} five steps of mass loss were observed in the temperature range 298–873 K (Fig. 5).

Table 2 Results from TG/DTG (2 K min^{-1}) and DSC (10 K min^{-1}) curves for RE(pic)$_3$2Leu·5H$_2$O compounds

RE	Step 1 298–403 K				Step 2 443–513 K				Step 3 513–593 K				Step 4 593–673 K		Step 5 673–1173 K	
	TG	DTG	DSC		TG	DTG	DSC		TG	DTG	DSC		TG	DTG	TG	DTG
	Δm/%	T/K	T/K	ΔH/kJ mol^{-1}	Δm/%	T/K	T/K	ΔH/kJ mol^{-1}	Δm/%	T/K	T/K	ΔH/kJ mol^{-1}	Δm/%	T/K	Δm/%	T/K
La	7.7	326	64	364.6	16.5	478	494	–406.7	26.0	546	572	–1768.2	13.9	626	23.5	674
Ce	7.7	316	65	217.0	15.1	462	482	–454.9	22.5	537	555	–1307.0	40.4	598	–	–
Pr	7.6	325	75	324.9	17.5	471	499	–514.0	24.2	546	567	–1307.1	16.4	623	20.7	685
Nd	7.7	334	75	214.2	27.2	469	489	–543.1	16.7	547	560	–460.7	16.4	603	18.0	663
Sm	7.6	328	74	367.2	10.5	473	518	–173.2	21.7	555	585	–1639.3	20.9	599	20.9	686
Eu	7.7	322	73	228.4	16.3	477	498	–473.0	22.4	554	569	–1252.1	16.6	612	18.7	671
Gd	7.6	328	74	243.1	16.9	474	501	–429.4	23.4	550	572	–1189.1	16.5	627	20.1	693
Tb	8.0	335	70	199.2	17.0	478	503	–390.1	22.8	556	576	–1370.5	18.1	625	19.1	697
Dy	7.6	329	79	202.5	16.7	478	502	–426.6	24.1	552	574	–1191.1	17.8	631	17.5	705
Ho	7.8	335	81	291.9	16.9	478	501	–503.8	23.5	554	577	–1304.0	16.4	630	19.4	694
Er	7.6	339	79	294.7	17.0	480	499	–447.3	22.4	557	572	–1141.1	18.8	629	18.8	704
Tm	7.5	332	83	235.3	17.4	479	503	–517.3	23.9	553	578	–1361.0	17.9	631	17.5	705
Yb	7.1	334	78	274.7	17.9	477	500	–476.6	22.8	552	573	–1134.0	18.0	636	17.9	723
Lu	7.7	336	78	226.6	17.4	476	500	–407.9	22.8	551	576	–1157.5	18.4	634	18.9	716
Y	8.2	333	84	240.4	18.4	475	498	–432.4	25.6	552	573	–1074.1	18.1	625	18.9	701

T = peak temperature, Δm = mass loss

Acknowledgements

The authors acknowledge Fundação de Amparo à Pesquisa do Estado de São Paulo (FAPESP) and Conselho Nacional de Desenvolvimento Científico e Tecnológico (CNPq) for financial support. One of us (TMS) is indebted to FAPESP for a doctoral fellowship (process 01/06684-1). The authors thank Prof. Dr. Hermi F. Brito and Dr. Ercules E. S. Teotonio for the recording of luminescence spectra.

References

1 T. S. Martins and P. C. Isolani, Quim. Nova, 28 (2005) 111.
2 J. B. Domingos, E. Longhinotti, V. G. Machado and F. Nome, Quim. Nova, 26 (2003) 745.
3 P. Maestro and D. Huguenin, J. Alloys Compd., 225 (1995) 520.
4 G. L. Baugis, H. F. Brito, W. Oliveira, F. R. Castro and S.-A. E. Falabella, Microporous Mesoporous Mater., 49 (2001) 179.
5 R. S. Puche and P. Caro, Rare Earths – Cursos de Verano de El Escorial, Editorial Complutense, Madrid 1998.
6 J. M. D. Coey, J. Magn. Magn. Mater., 248 (2002) 441.
7 V. Zezulka, P. Straka and P. Mucha, J. Magn. Magn. Mater., 268 (2004) 219.
8 G. Blasse and B. C. Grabmaier, Luminescent Materials, Springer-Verlag, Berlin Heidelberg 1994.
9 C. R. Ronda, T. Jüstel and H. Nikol, J. Alloys Compd., 275 (1998) 669.
10 B. Moine and G. Bizarri, Mater. Sci. Eng., B105 (2003) 2.
11 C. A. Kodaira, H. F. Brito and M. C. F. C. Felinto, J. Solid State Chem., 171 (2003) 401.
12 R. Reisfeld, Inorg. Chim. Acta, 140 (1987) 345.
13 K. Kuriki, Y. Koike and Y. Okamoto, Chem. Rev., 102 (2002) 2347.
14 H. Jiang, J. Wang, X. Hu, H. Liu, C. Zhang, B. Teng and J. Li, J. Cryst. Growth, 234 (2002) 699.
15 J.-C. G. Bünzli and G.R. Choppin, Lanthanide Probes in Life, Chemical and Earth Sciences, Theory and Practice, Elsevier, Amsterdam, Oxford, New York 1989.
16 M. Elbanowski and B. Makowska, J. Photochem. Photobiol., A: Chem., 99 (1996) 85.
17 I. Hemmilä, J. Alloys Compd., 225 (1995) 480.
18 G. Bombieri and R. Artali, J. Alloys Compd., 344 (2002) 9.
19 T. M. Corneillie, P. A. Whetstone, A. J. Fisher and C. F. Meares, J. Am. Chem. Soc., 125 (2003) 3436.
20 T. S. Martins, A. A. S. Araújo, M. P. B. M. Araújo, P. C. Isolani and G. Vicentini, J. Alloys Compd., 344 (2002) 75.
21 T. S. Martins, A. A. S. Araújo, S. M. da Silva, J. R. Matos, P. C. Isolani and G. Vicentini, J. Solid State Chem., 171 (2003) 212.
22 T. Glowiak, J. Legendziewicz, E. Huskowska and P. Gawryszewska, Polyhedron, 15 (1996) 2939.
23 P. Indrasenan and M. Lakshmy, Indian J. Chem., 36A (1997) 998.
24 J. Torres, C. Kremer, H. Pardo, L. Suescun, A. Mombrú, J. Castiglioni, Sixto Domínguez, A. Mederos and E. Kremer, J. Mol. Struct., 660 (2003) 99.
25 J. Legendziewicz, T. Glowiak and E. Huskowska, Polyhedron, 8 (1989) 2139.
26 K. Umeda, P. C. Isolani, M. H. Zaim and G. Vicentini, J. Alloys Compd., 344 (2002) 80.
27 M. C. C. Cardoso, D. M. Araújo Melo, J. Zukerman- Schpector, L. B. Zinner and G. Vicentini, J. Alloys Compd., 344 (2002) 83.
28 E. P. Marinho, W. S. C. de Sousa, D. M. A. Melo, L. B. Zinner, K. Zinner, L. P. Mercuri and G. Vicentini, Thermochim. Acta, 344 (2000) 67.
29 C. C. F. Nunes, K. Zinner, L. B. Zinner, C. C. Carvalho, J. Zukerman-Schpector and G. Vicentini, Inorg. Chim. Acta, 292 (1999) 249.
30 C. V. P. de Melo, G. Vicentini, P. C. Isolani, J. Zukerman-Schpector and E. E. Castellano, J. Alloys Compd., 277 (1998) 242.
31 S. A. Jardino Filho, P. C. Isolani and G. Vicentini, J. Alloys Compd., 249 (1997) 91.
32 E. P. Marinho, D. M. A. Melo, L. B. Zinner, K. Zinner, E. E. Castellano, J. Zukerman-Schpector, P. C. Isolani and G. Vicentini, Polyhedron, 16 (1997) 3519.
33 T. S. Martins, J. R. Matos, G. Vicentini and P. C. Isolani, J. Therm. Anal. Cal., 82 (2005) 77.
34 P. Schauder, J. Wahren, R. Paoletti, R. Bernardi and M. Rinetti, Branched-Chain Amino Acids. Biochemistry, Physiopathology and Clinical Science, Raven Press, New York 1992.
35 D. Voet, J. G. Voet and C. W. Pratt, Fundamentos de Bioquimica, Artemed Editora, Porto Alegre 2002.
36 S. J. Lyle and M. M. Rahman, Talanta, 10 (1963) 1177.
37 W. J. Geary, Coord. Chem. Rev., 7 (1971) 81.
38 A. Barth, Progress in Biophys. Mol. Biol., 74 (2000) 141.
39 K. Nakamoto, Infrared spectra of inorganic and coordination compounds, second edition, New York 1969.
40 M. T. Rosado, M. L. T. S. Duarte and R. Fausto, Vib. Spectrosc., 16 (1998) 35.
41 G. W. Watt and J. F. Knifton, Inorg. Chem., 6 (1967) 1010.
42 E. P. P. Agnes, Anal. Chem., 29 (1957) 1283.
43 M. L. Bair and E. M. Larsen, J. Am. Chem. Soc., 93 (1971) 1140.
44 D. D. McCraken and W. S. Dorn, Numerical Methods and Fortran Programming, Wiley, New York 1966.
45 P. Porcher and P. Caro, Seminaires de Chime de L'État Solid, 5 (1972) 141.
46 P. P. Gawryszewka, L. Jerzykiewicz, P. Sobota and J. Legendziewicz, J. Alloys Compd., 300 (2000) 275.

Received: September 2, 2005
Accepted: November 2, 2005
OnlineFirst: May 23, 2006

DOI: 10.1007/s10973-005-7309-0